

Supplementary Material

Improvement on the Use of Se@C in Batteries by Synergistic Effect of Nano-Confinement and C-Se Bond

Lijun Wu ^{1,2}, Shoujie Guo ¹, Hongwei Yue ¹, Hao Li ¹, Wei Li ¹, Chuan Yao ¹, Pinjiang Li ¹, Wenjun Fa ¹, Burong Song ¹, Kai Li ¹, Bitao Zhou ¹, Qian Yu ¹, Yunjun Xu ³, Changchun Yang ^{1,*}, Zhi Zheng ^{1,*} and Yuanhao Gao ^{1,*}

- ¹ Henan Provincial Key Laboratory of Micro and Nano Energy Storage and Conversion Materials, Henan Provincial Engineering Laboratory of Micro and Nano Energy Materials and Devices, and Henan International Joint Laboratory of Nano Energy and Catalytic Materials, Xuchang University, Xuchang 461002, China
² Guangxi Key Laboratory of Electrochemical Energy Materials, Guangxi University, Nanning 530004, China
³ Henan Kelong New Energy Co., Ltd., Xinxiang 453000, China
* Correspondence: changchun@zzu.edu.cn (C.Y.); zhengzhi99999@gmail.com (Z.Z.); gyh-2007@sohu.com (Y.G.)

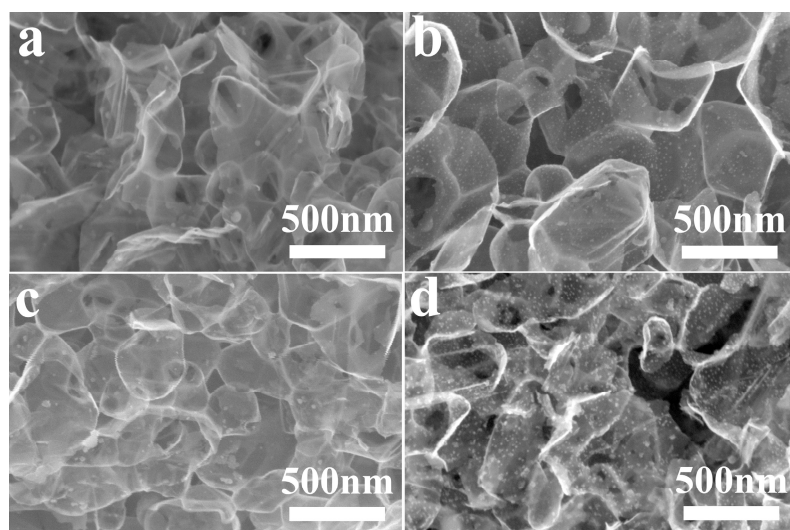


Figure S1. Low-resolution images of FESEM for Se@SCDC with various mass ratios of Se/C: (a) $m_{Se}/m_C = 4/1$; (b) $m_{Se}/m_C = 5/1$; (c) $m_{Se}/m_C = 6/1$; (d) $m_{Se}/m_C = 7/1$.

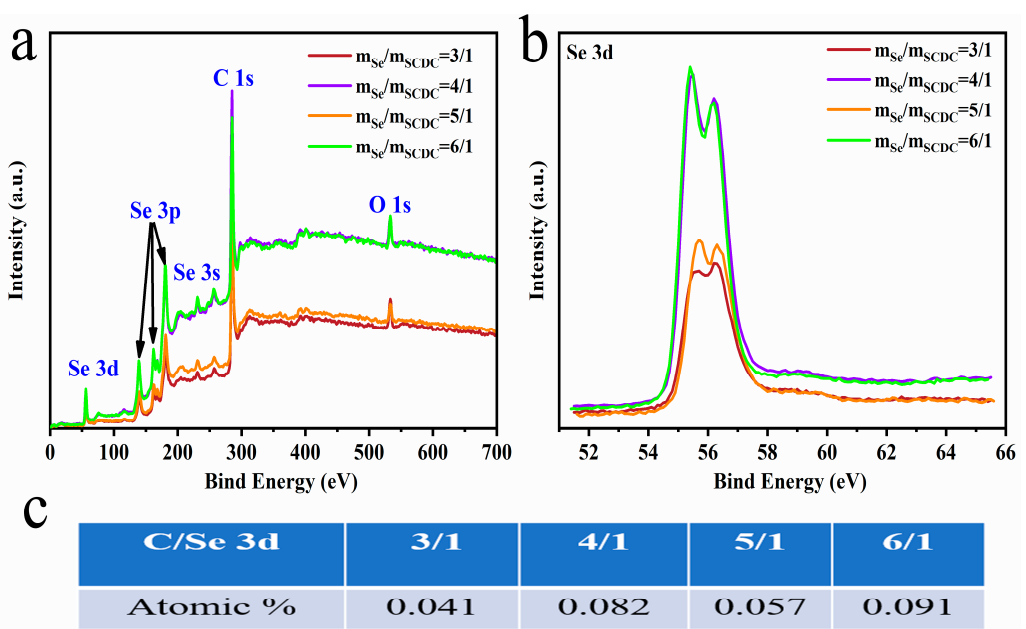
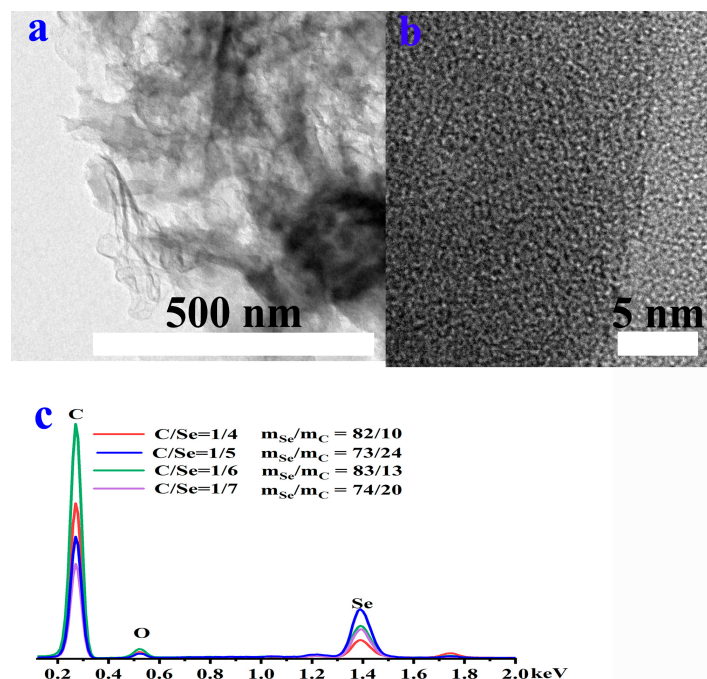


Figure S3. (a) the XPS survey; (b) Se 3d spectrum and (c) the ratio of atomic% for SCDC/Se of Se@SCDC materials with $m_{\text{Se}}/m_{\text{C}} = 3/1$; $m_{\text{Se}}/m_{\text{C}} = 4/1$; $m_{\text{Se}}/m_{\text{C}} = 5/1$ and $m_{\text{Se}}/m_{\text{C}} = 6/1$.

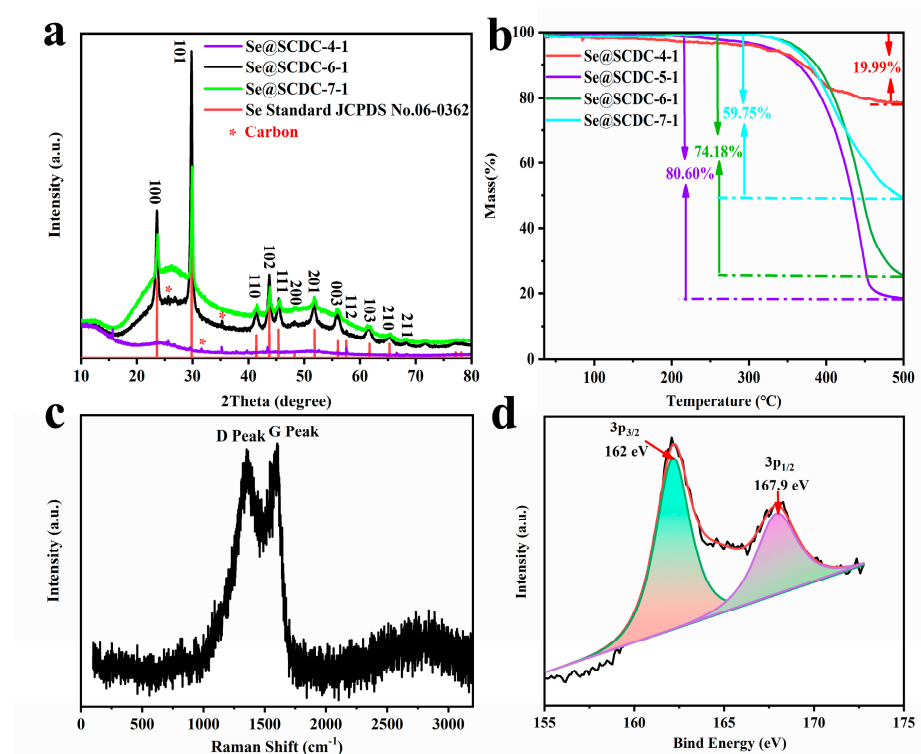


Figure S4. (a) X-ray diffraction of Se and Se@SCDC materials with different mass ratios of Se/C; (b) Thermogravimetric Analysis of Se@SCDC materials with different mass ratios of Se/C; (c) the Raman spectra of SCDC; (d) the high-resolution XPS spectrum of Se 3p.

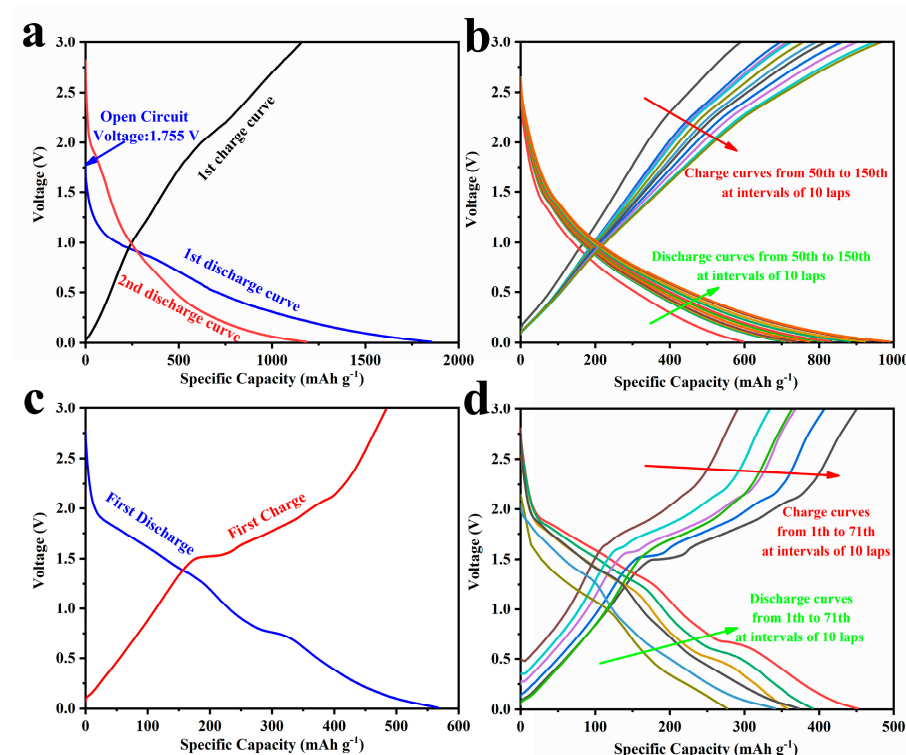


Figure S5. the voltage-specific capacity curves of Se@SCDC-5-1/Li (a) initial cycles; (b) from 50th to 150th at 0.1 A g^{-1} ; (c) first charge and discharge curves and (d) the voltage-specific capacity curves of Se@SCDC-5-1/Na corresponds to gradient charge/discharge rates of Se@SCDC-5-1 composite from 0.1, 0.2, 0.5, 1.0, 2.0 to 5.0 A g^{-1} inset Figure 4c of the manuscript.

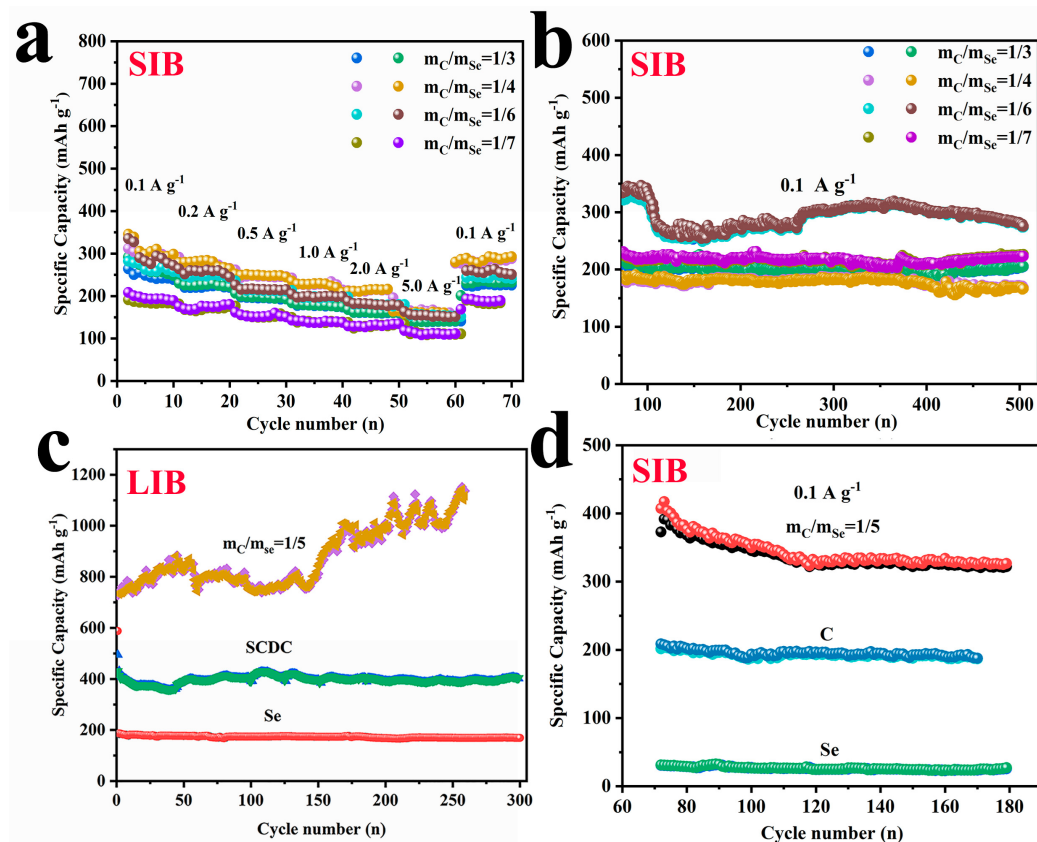


Figure S6. (a) Gradient charge-discharge characteristic of Se@SCDC with various mass ratios of Se@SCDC/Na; (b) Cyclic stability at 0.1 A g⁻¹ of Se@SCDC/Na with various mass ratios of Se@SCDC; (c) Cyclic stability at 0.1 A g⁻¹ of Se@SCDC, C or Se/Li; (d) Cyclic stability at 0.1 A g⁻¹ of Se@SCDC, C or Se/Na.

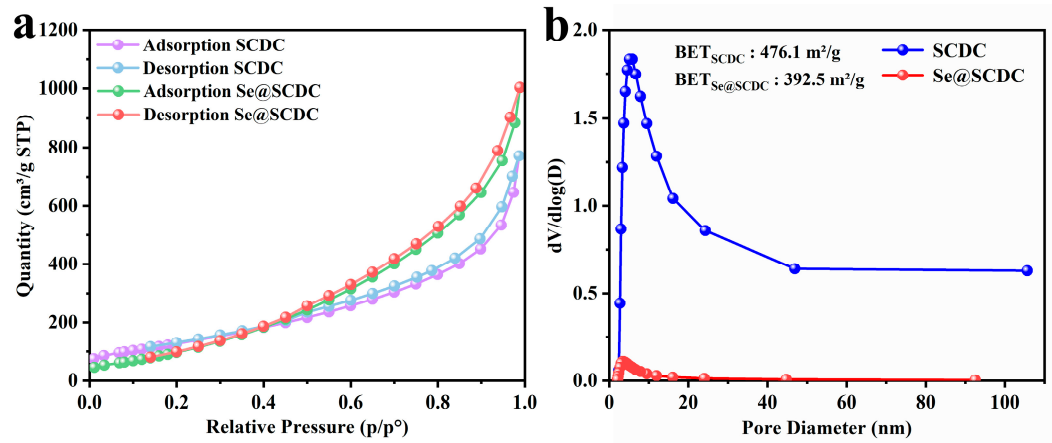


Figure S7. (a) The adsorption and desorption isothermal curves and (b) pore size distribution of SCDC and Se@SCDC materials.

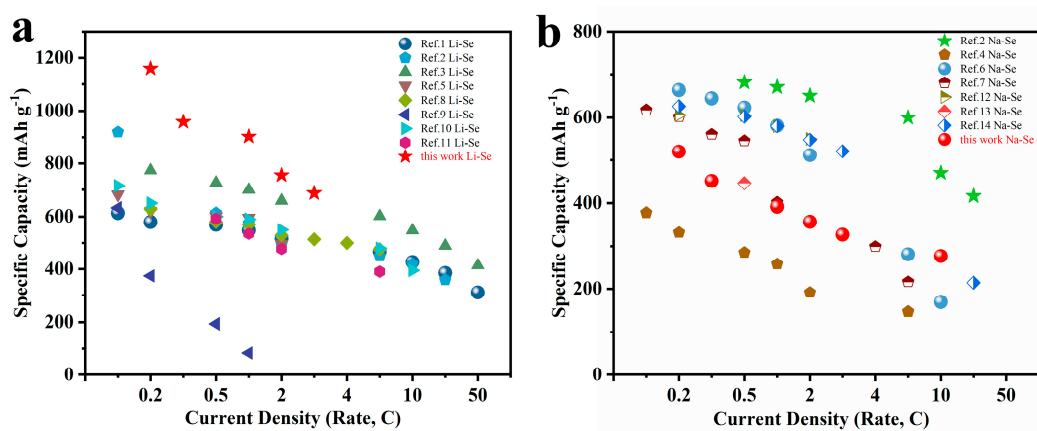


Figure S8. Comparison of (a) lithium and (b)sodium storage performance for Se@SCDC material and other materials.

References

- Tian, H.; Tian, H.; Wang, S.; Chen, S.; Zhang, F.; Song, L.; Liu, H.; Liu, J.; Wang, G. High-Power Lithium-Selenium Batteries Enabled by Atomic Cobalt Electrocatalyst in Hollow Carbon Cathode. *Nat Commun.* **2020**, *11*, 5025. DOI: 10.1038/s41467-020-18820-y
- Zhao, X.; Yin, L.; Zhang, T.; Zhang, M.; Fang, Z.; Wang, C.; Wei, Y.; Chen, G.; Zhang, D.; Sun, Z. and Li, F. Heteroatoms Dual-Doped Hierarchical Porous Carbon-Selenium Composite for Durable Li-Se and Na-Se Batteries. *Nano Energy* **2018**, *49*, 137–146. DOI: 10.1016/j.nanoen.2018.04.045
- Zhou, J.; Chen, M.; Wang, T.; Li, S.; Zhang, Q.; Zhang, M.; Xu, H.; Liu, J.; Liang, J.; Zhu, J. and Duan, X. Covalent Selenium Embedded in Hierarchical Carbon Nanofibers for Ultra-High Areal Capacity Li-Se Batteries. *iSci.* **2020**, *23*, 100919. DOI: 10.1016/j.isci.2020.100919
- Sun, W.; Guo, K.; Fan, J.; Min, Y. et al. Confined Selenium in N-Doped Mesoporous Carbon Nanospheres for Sodium-Ion Batteries. *ACS Appl. Mater. Interf.* **2021**, *13*, 16558–16566. DOI: 10.1021/acsami.1c02842
- Hong, Y.; Kang, Y. Selenium-Impregnated Hollow Carbon Microspheres as Efficient Cathode Materials for Lithium-Selenium Batteries. *Carbon*, **2017**, *111*, 198–206. DOI: 10.1016/j.carbon.2016.09.069
- Kim, J.; Kang, Y. Encapsulation of Se into Hierarchically Porous Carbon Microspheres with Optimized Pore Structure for Advanced Na-Se and K-Se Batteries. *ACS Nano*, **2020**, *14*(10), 13203–13216. DOI: 10.1021/acsnano.0c04870
- Zhao, D.; Wang, L.; Qiu, M. and Zhang, N. Amorphous Se Restrained by Biomass-Derived Defective Carbon for Stable Na-Se Batteries. *ACS Appl. Energy Mater.* **2021**, *4*(7), 7219–7225. DOI: 10.1021/acsadm.1c01317
- Wang, B.; Zhang, J.; Xia, Z.; Fan, M.; Lv, C.; Guanglei, Tian, G. and Xiaona, Li. Polyaniline-coated selenium/carbon composites encapsulated in graphene as efficient cathodes for Li-Se batteries. *Nano Res.* **2018**, *11*, 2460–2469. DOI: 10.1007/s12274-017-1870-2
- Mukkabla, R.; Deshagani, S.; Meduri, P.; Deepa, M. and Ghosal, P. Selenium/Graphite Platelet Nanofiber Composite for Durable Li-Se Batteries. *ACS Energy Lett.* **2017**, *2*(6), 1288–1295. DOI: 10.1021/acsenergylett.7b00251
- Zhang, S.; Wang, W.; Xin, S.; Ye, H.; Yin, Y.; and Guo, Y. Graphitic Nanocarbon-Selenium Cathode with Favorable Rate Capability for Li-Se Batteries. *ACS Appl. Mater. Interfaces*, **2017**, *9*(10), 8759–8765. DOI: 10.1021/acsami.6b16708
- Feng, N.; Xiang, K.; Xiao, L.; Chen, W.; Zhu, Y.; Liao, H. and Chen, H. Se/CNTs microspheres as improved performance for cathodes in Li-Se batteries. *J. Alloy Compd.*, **2019**, *786*, 537–543. DOI: 10.1016/j.jallcom.2019.01.348.
- Dong, W.; Wang, C.; Li, C.; Xia, F.; Yu, W.; Wu, L.; Mohamed, H.; Hu, Z.; Liu, J.; Chen, L.; Li, Y. and Su, B. The free-standing N-doped Murray carbon framework with the engineered quasi-optimal Se/C interface for high-Se-loading Li/Na-Se batteries at elevated temperature. *Mater. Today Energy*, **2021**, *21*, 100808. DOI: 10.1016/j.mtener.2021.100808
- Wu, X.; Chen, X.; Wu, H.; Xie, B.; Wang, D.; Wang, R.; Zhang, X.; Piao, Y.; Diao, G. and Chen, M. Encapsulation of Se in dual-wall hollow carbon spheres: Physical confinement and chemisorption for superior Na-Se and K-Se batteries. *Carbon*, **2022**, *187*, 354–364. DOI: 10.1016/j.carbon.2021.11.013
- Kim, J.; Kang, Y. Deliberate introduction of mesopores into microporous activated carbon toward efficient Se cathode of Na-Se batteries. *INT J ENERG RES*, **2022**, *46*(3), 3396–3408. DOI: 10.1002/er.7389

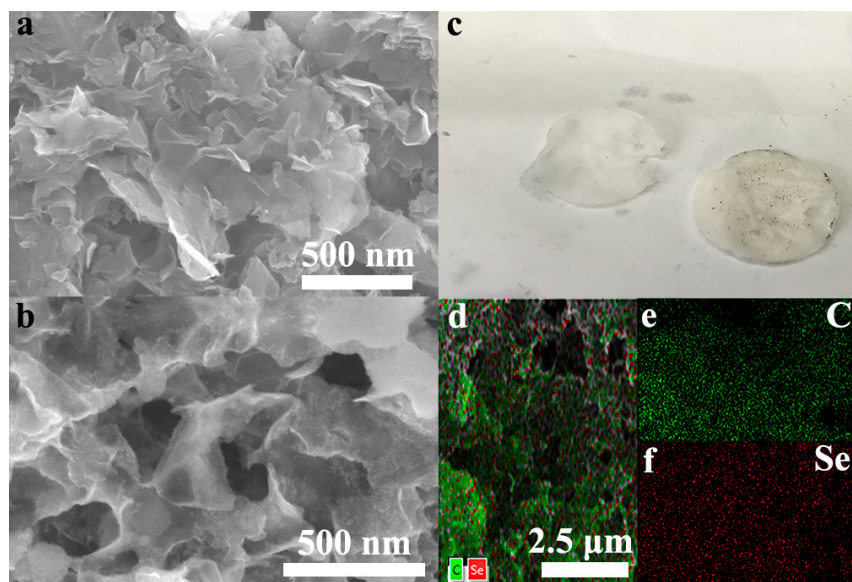


Figure S9. *Ex-situ* SEM (a) before and (b) after 100 cycles; (c) The optical photograph of electrolyte; (d) the electron diffraction energy spectrum (EDS) determined by FESEM; element distribution map of (e) C and (f) Se of Se@SCDC-5-1/Na after 100 cycles.